

# **Tectonics of Kachchh basin based on field structural geological studies and paleostress analysis in Bhuj, Gujarat, India**

A Thesis

submitted to

Indian Institute of Science Education and Research Pune in partial  
fulfilment of the requirements for the BS-MS Dual Degree Programme

by

**MS Dhawale**



Indian Institute of Science Education and Research Pune

Dr. Homi Bhabha Road,

Pashan, Pune 411008, INDIA.

October 20, 2020

Supervisor: Dr. Soumyajit Mukherjee

© MS Dhawale 2020

All rights reserved

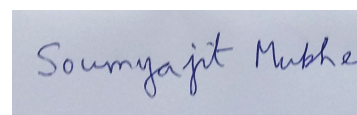


# Certificate

This is to certify that this dissertation entitled '**Tectonics of Kachchh basin based on field structural geological studies and paleostress analysis in Bhuj, Gujarat, India**' towards the partial fulfilment of the BS-MS dual degree programme at the Indian Institute of Science Education and Research, Pune represents study/work carried out by **MS Dhawale** at Indian Institute of Technology Bombay under the supervision of **Dr. Soumyajit Mukherjee**, Associate Professor, Department of Earth Sciences, IIT Bombay, during the academic year 2019-2020.



MS Dhawale



Dr. Soumyajit Mukherjee

Committee:

Dr. Soumyajit Mukherjee

Dr. Sudipta Sarkar

This thesis is dedicated to all medical professionals and front-line workers in COVID-19 global pandemic.

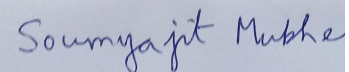
# Declaration

I hereby declare that the matter embodied in the report entitled '**Tectonics of Kachchh basin based on field structural geological studies and paleostress analysis in Bhuj, Gujarat, India**' are the results of the work carried out by me at the Department of Earth Sciences, Indian Institute of Technology Bombay, under the supervision of **Dr. Soumyajit Mukherjee** and the same has not been submitted elsewhere for any other degree.



MS Dhawale

Date: 22 / 10 / 2020



Dr Soumyajit Mukherjee

# Abstract

The Mesozoic Kachchh basin is one of the most active tectonic and seismological regions in India in NW Gujarat. The tectonic setting here comprises of many regional faults and movement along these faults frequently result in seismicity. This thesis comprises of understanding the formation of some of these faults and the paleostress analysis along those fault planes. The stress analyses provided paleostress axes orientations from the selected areas of study around the Bhuj city.

The fault systems observed in this study are used for performing paleostress analysis. The results of this analysis shows that the terrain is primarily under extensional stress and thus the rocks are faulted normally. A total number of 94 data points were analyzed from 5 different sites. The direction of principle stress axes for studied sites is ~NE for maximum stress axis and ~SW for minimum stress axis. The results from both programs used for analysis are similar and show similar trend. The direction of stress axes and that of extension obtained from the programs match the overall trend in Kachchh Rift Basin (KRB) and thus confirm that the findings of the study are compatible with the surroundings.

# Acknowledgments

I am grateful to my project supervisor, **Dr. Soumyajit Mukherjee (IIT Bombay)** for his guidance throughout the project and for availing me registered software programs that were necessary for this project. I thank **Dr. Sudipta Sarkar (IISER Pune)** for his administrative guidance at IISER Pune. I would like to specially thank **Dr. Dripta Datta (IIT Kanpur)** for patiently solving my doubts about the programs and helping me with the operations. I would like to thank **Mr. Haroon Shaikh (MSU Baroda)** for his annotations and advises on my reports and thesis. I would also like to thank **Md. Walid** and **Nupur Pant (IIT Bombay)**, and **Nidhi Lohani** and **Aashu Pawar (Panjab University)** for their inputs during lab and online discussions. I would like to specially thank **Md. Walid** for providing me accommodation during my project at IIT Bombay.

I would like to thank Department of Science and Technology, Government of India for providing me financial assistance through INSPIRE fellowship during the course of this project. I am indebted to **Dr. Sudipta Sarkar (IISER Pune)** for his help about mid term presentation and thesis submission. **Dr. Supriya Pisolkar (IISER Pune)** is thanked for her support and providing information on submission deadlines and other important dates. I would also like to thank administration of IIT Bombay for providing me access to on campus facilities e.g. hostel and gymkhana during my stay at the Institute.

# Table of Contents

<b>Abstract</b> .....	<b>VI</b>
<b>Acknowledgments</b> .....	<b>VII</b>
<b>List of abbreviations</b> .....	<b>01</b>
<b>List of tables</b> .....	<b>03</b>
<b>List of figures</b> .....	<b>04</b>
<b>Chapter 1</b>	
<b>Introduction</b> .....	<b>05</b>
1.1 Structural deformations observed in Kachchh.....	05
1.2 Geology of Kachchh.....	09
1.3 Tectonic setting of Kachchh.....	11
<b>Chapter 2</b>	
<b>Methodology</b> .....	<b>15</b>
2.1 Data sampling and Documentation.....	15
2.2 Paleostress and inversion analysis.....	18
<b>Chapter 3</b>	
<b>Results</b> .....	<b>21</b>
3.1 Results from T-TECTO.....	21
3.2 Results from Win_Tensor.....	25
<b>Chapter 4</b>	
<b>Discussions</b> .....	<b>30</b>
4.1 Comparative analysis of results from T-TECTO and Win_Tensor...	30



4.2	Stress Ratio and Stress Regime.....	31	
4.3	Stress regime and Fault formation timeline.....	33	
<b>Chapter 5</b>			
<b>Conclusions.....</b>			<b>36</b>
<b>Appendix A.....</b>			<b>37</b>
	T-TECTO.....	37	
	Win_Tensor.....	37	
<b>Appendix B.....</b>			<b>39</b>
<b>References.....</b>			<b>44</b>

# List of Abbreviations

ABF	Allah Bund Fault
BF	Banni Fault
BU	Bela Uplift
CU	Chorar Uplift
DU	Desalpar Uplift
GDF	Gora Dungar Fault
GF	Gedi Fault
IBF	Island Belt Fault
IBU	Island Belt Uplift
KHF	Katrol Hill Fault
KHRFZ	Katrol Hill Range Fault Zone
KMF	Kachchh Mainland Fault
KMU	Kachchh Mainland Uplift
KRB	Kachchh Rift Basin
KU	Khadir Uplift
MSM	Multiple Slip Method
NHRFZ	Northern Hill Range Fault Zone
NKF	North Kathiawar Fault
NPF	Nagar Parkar Fault
NPU	Nagar Parkar Uplift
NWF	North Wagad Fault
PU	Pachcham Uplift

RDM	Right Dihedra Method
SWF	South Wagad Fault
VGKF	Vigodi-Katrol Fault
VGKNFS	Vigodi-Gugriana-Khirasra-Netra Fault System
WU	Wagad Uplift

# List of Tables

3.1	Results of inversion analysis from T-TECTO.....	25
3.2	Results of inversion analysis from Win_Tensor.....	29
4.1	Comparative analysis of stress axes orientations.....	30
4.2	Stress regime type variation.....	33
A1	Format code for data entry in Win_Tensor.....	38
B1	Fault slip data for Area E.....	39
B2	Fault slip data for Area K.....	40
B3	Fault slip data for Area M.....	41
B4	Fault slip data for Area N.....	42
B5	Fault slip data for Area O.....	43

# List of Figures

1.1	Deformation structures in Kachchh.....	07
1.2	Erosional structures in Kachchh.....	07
1.3	Types of Faults.....	07
1.4	Fault planes and slickenlines.....	09
1.5	Geological map of Kachchh.....	11
1.6	Tectonic setting of Kachchh.....	13
2.1	Clinometer.....	17
2.2	Locations of data acquisition sites.....	18
3.1	Results of T-TECTO from Area E.....	22
3.2	Results of T-TECTO from Area K.....	23
3.3	Results of T-TECTO from Area M.....	23
3.4	Results of T-TECTO from Area N.....	24
3.5	Results of T-TECTO from Area O.....	24
3.6	Results of Win_Tensor from Area E.....	26
3.7	Results of Win_Tensor from Area K.....	27
3.8	Results of Win_Tensor from Area M.....	27
3.9	Results of Win_Tensor from Area N.....	28
3.10	Results of Win_Tensor from Area O.....	28
4.1	Types of stress regimes.....	32

# Chapter 1

## Introduction

Structural geology is a branch of geological science that deals with deformation of rocks in various ways. The scope of such a study is vast in scale as the deformations in rocks can be as small as a few micrometers to hundreds of kilometers (Fossen, 2016). The types of rock structures observed in nature and stresses acting on them result in variety of deformations. This study deals with the various types of structures observed in nature and their possible formation mechanisms.

### 1.1 Structural deformations observed in Kachchh

A lot of geological features were observed and noted in Kachchh along with data sampling during the field trip to the study site. Some of the fundamental deformation structures observed in Kachchh are folds, faults, joints, and various patterns due to sedimentation, erosion, and weathering. A few of these structures are as described below.

#### 1.1.1 Fractures

Breaking of a rock body along a weak plane with or without any relative movement along the breakage is called a fracture (Rey, 2016). If there is relative movement along the plane of breaking, it is called as a fault and if there is no movement along the plane then it is called a joint. Some of the fractured rock bodies observed in the study area are shown below in Fig. 1.1 (a).

#### 1.1.2 Veins

Vein is a structure that is formed by sheetlike crystallization of minerals in rock fractures (Rey, 2016). When minerals are precipitated along narrow fractures in rock

bodies they over time form crystals on the walls of fractures and grow normal to it protruding in open space. Usually these veins are micrometers to a few millimeters wide. The two mechanisms with which veins are formed are Open space filling and Crack seal method (Bons, 2000). Open space filling occurs when the confining pressure is low and it is a slow process. Crack Seal method however is rapid and occurs when confining pressure is high. As veins form in preexisting fractures, their density is naturally high in brittle rocks and less in undeformed rocks. Fig. 1.1 (b) shows the veins observed in the study area and their networks.

### **1.1.3 Paleo-current indicators**

Paleo-current indicators are those sedimentary structures that help to understand the direction of flowing water in past. They are a result of hydrodynamics and interaction of flowing water and sediment at the past sediment water interface. For example, the foresets of a migrating ripple can serve as paleo-current indicator. A clear demarcation of the topset, foreset and bottomset and the angularity of the foreset with the overlying and underlying bedsets help to understand the flow direction. An observed pattern of paleo-current indicator, such as a foresets of ripple in Kachchh is shown in Fig. 1.2 (a).

### **1.1.4 River Gorge**

When fast moving river is obstructed by a hard rock body, the rock is eroded over time and the depth of river keeps increasing. It results in deep and narrow valleys with multiple curves along the walls. The Khari Nadi, flowing from the western outskirts of Bhuj city, Gujarat has formed such a gorge which is visible from bridge on Kodki road. Fig. 1.2 (b) shows this gorge on the Khari Nadi.

### **1.1.5 Faults**

As introduced in fractures, when a rock body fractures and its both walls slip relative to each other, the deformation is called as fault (Rey, 2016). There are many kinds of faults depending upon the orientation and direction of slip. Faults are most widely classified as normal, reverse and strike-slip faults. Fig. 1.3 shows different types of faults along with the direction of slip. Most of the faults observed in and around Bhuj were normal faults along with strike slip. Kachchh is a tectonically active region and hence fault density in the study area is very high (Maurya, 2000). Therefore, the study area has great potential for understanding the kinematics of rock deformations along with fault slip mechanisms.

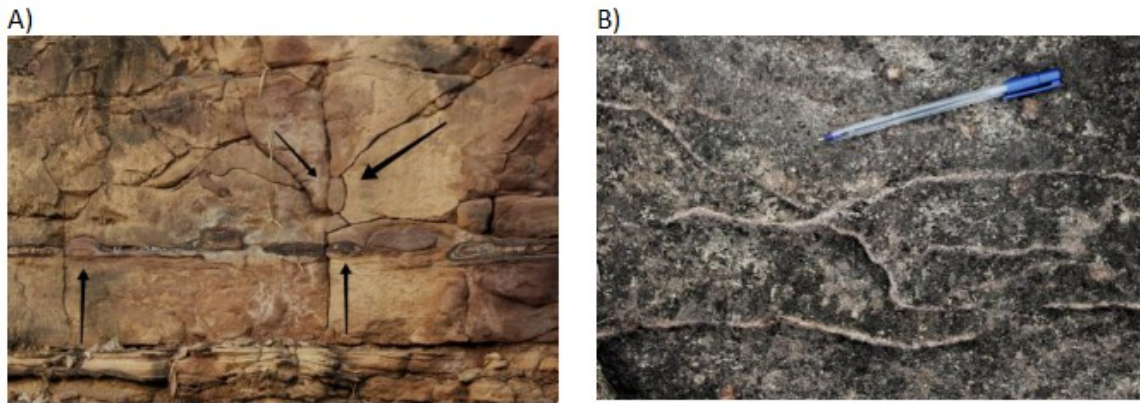


Fig. 1.1: A) Fractures observed and marked with black arrows on a cropped out rock alongside Airport road, Bhuj. B) Vein network formed on hillock formed by fault on Kodki road, Bhuj.

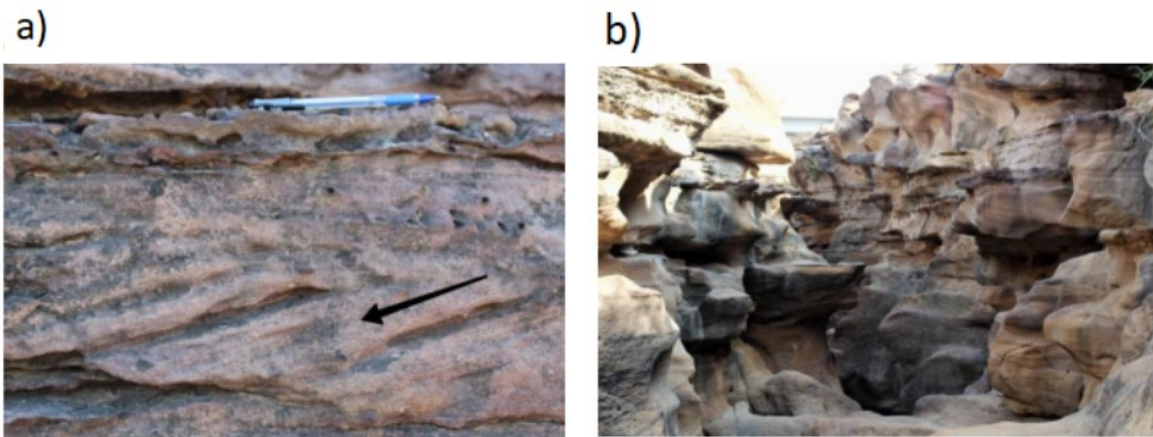


Fig. 1.2: A) Paleo-current indicator with direction of flow indicated with black arrow spotted on vertical section of fault on Kodki road, Bhuj. B) River gorge on Khari Nadi in western outskirts of Bhuj.

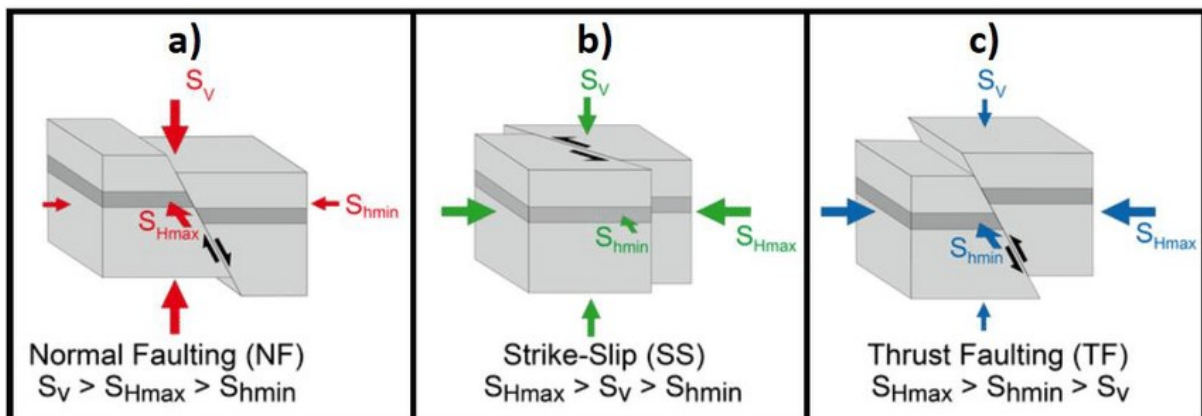


Fig. 1.3: Different types of faults a) normal, b) strike-slip, c) reverse/thrust.  $S_{Hmax}$  = Maximum Horizontal Stress,  $S_{hmin}$  = Minimum Horizontal Stress,  $S_v$  = Vertical Stress. Reproduced from Heidbach et. al. (2016).



### **1.1.6 Fault plane**

The plane of fracture on which walls of the rock body have slipped against each other is the fault plane. It can be traced by observing the discontinuation and movement of sedimentary beds or it can also be observed exposed as a cropped out structure (Rey, 2016). The fault plane is very distinguishing structure which as observed, usually exists in contrasting colour to that of the rock body. The plane, if exposed, has very smooth texture and can sometimes have slip direction indicators carved on them. Fig. 1.4 (a) and 1.4 (b) shows the traces of fault planes.

### **1.1.7 Slickenlines**

The slip direction indicator formed on the fault plane called slickenlines, also known as lineations, are formed because of friction between two walls of fractured rock, when they slipped past each other. These slickenlines are very useful in processing paleostress analysis which gives an understanding of deformational stresses acting in past. The slickenlines can be easily spotted on exposed fault planes as straight marked lines as shown in Fig. 1.4 (c). As observed in the field, the spotting becomes much easier when slickenlines are exposed to direct sunlight.



Fig. 1.4: A) Fault plane marked as black line by tracing termination of bands of sedimentation. B) Fault plane marked as black line traced by exposed cropped out part of the rock body. C) Slickensides marked as black line observed on the fault plane. All structures are spotted on Kodki road, Bhuj.

## 1.2 Geology of Kachchh

Located in west Gujarat and sharing political border with Pakistan, and the biggest district in India, Kachchh hosts diverse landscapes and sedimentary deposits. A major part of Kachchh is covered with the Rann of Kachchh, the great salt marsh and a flat land, but the remaining area is covered with highlands created with fault uplifts, Banni grasslands and coastal plain (Merh, 1995). The Kachchh district is in a shape of peninsula with the Great Rann of Kachchh in the north and Little Rann in

the east. Both of these are salt flats, composed of Quaternary clay and evaporate sediments (Mukherjee, 2018). Both Great and Little Rann of Kachchh are a part of Thar Desert in North-Western India extending up to South-East Pakistan. The outcropped geological highlands are bounded by major fault systems observed throughout Kachchh. Kachchh represents perpendicular to west Indian margin, a fossil rift basin which contain sedimentary deposits of late Triassic sands on Precambrian rocks.

One of the hypothesis on the formation of Kachchh basin is that it is supposed to be formed by the breakup of Gondwanaland in the Mesozoic period and thus, the existence of Mesozoic sediments in Kachchh is explained. The breakup resulted in extensional stress in the basin causing multiple normal faults in the region (Sen et. al., 2019). After collision with the Eurasian plate, the rift basin's extensional regime converted in N-S compression at around  $55 \pm 1$  Ma. The observed reverse faults in the basin are a result of this compressional stress (Maurya et. al., 2016). As the compression was N-S trending, the reverse faulting was predominant in E-W direction. The plate boundaries of Eurasian and Arabian Plate met that of Indian plate fractured from Gondwanaland and formed a triple junction at the west of Indian plate. This vicinity of triple junction and high regional stress field due to it resulted in high seismic activity in the Kachchh basin (Chopra et. al., 2013). The kinematics at these plate boundaries and triple junction also affect the tectonics of Kachchh basin.

The study area chosen for fault slip analysis was near the city of Bhuj, in central part of Kachchh basin. This area is uplifted due to Kutch Mainland Uplift (KMU). Bhuj city and its outskirts consists mainly of Mesozoic sediments. But along with these Mesozoic rocks, there are some Cenozoic sedimentary deposits observed with interventions of Deccan trap volcanics. Cities like Jhurio, Jhuran and Bhuj consists of Mesozoic sequence (Sen et. al., 2019). After the Mesozoic rift sedimentation, Deccan trap eruptions occurred. The movement along the faults resulted in intrabasinal uplifts. The fault reactivation in Kachchh basin is periodically testified by Cenozoic sediments in structural lows, fault controlled current landscape and seismicity (Sarkar et. al., 2007). The southern part of KMU is formed by an arc of Mesozoic sediments that surrounds the Bhuj city. Surrounding this Mesozoic sequence, is Deccan trap intrusions and sedimentation in further southward part of the basin is dominated by Tertiary sediments. The coastal region consists of Quaternary sediments (Merh, 1995). The northern part of Kutch Mainland Fault

(KMF) which covers the significant part of The Great Rann of Kachchh also consists of Quaternary sediments. Pachcham, Khadir, Bela and Chorar uplifted islands which are further northward are formed by Mesozoic sequence with some Deccan traps. Wagad uplift in eastern Kachchh also shows similar geology with Mesozoic sediments and Deccan trap intrusions (Singh and Mandal, 2020). Limestone, Shale and Sandstone are the most common rocks in Kachchh basin. Some fossiliferous Eocene and Jurassic rocks are found in south central Kachchh that are exposed in south Kachchh peninsular region as a thin band (Mukherjee, 2018). The city of Bhuj and its surroundings consists of sandstone and shale with traces of plant of fossils in between. The vertical crop out sections in outskirts of Bhuj city give a good opportunity for study of geological structures and sedimentary deposits in the area.

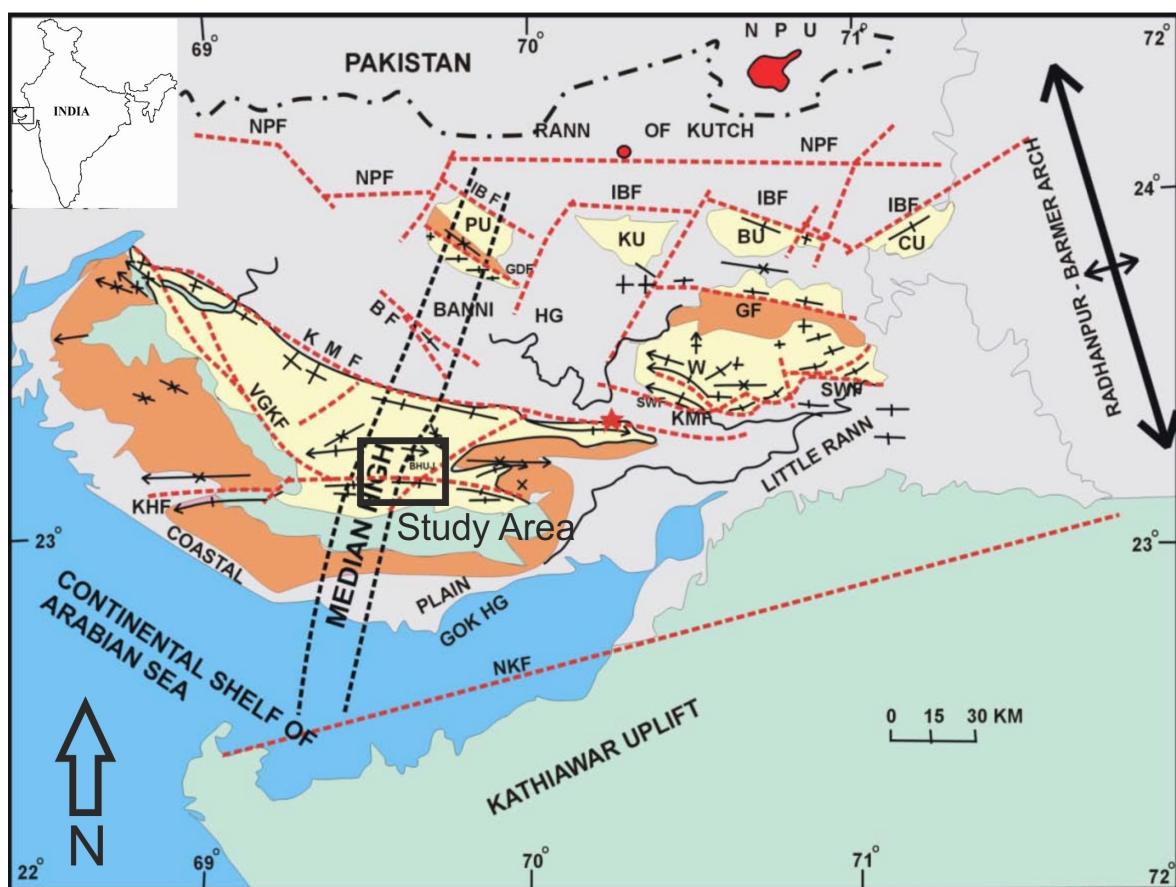


Fig. 1.5: Geological map of Kachchh, reproduced from Biswas (2005).

### 1.3 Tectonic Setting of Kachchh

Bhuj is situated in central Kachchh which is a tectonically active region. Kachchh basin is highlighted as seismically most active region in India along with Himalayas. This active tectonics and high seismicity can be reasoned with vicinity of

triple junction of Indian, Eurasian and Arabian plate (Chopra et. al., 2013). The entire Kachchh region has been modified several times due to various earthquakes and its active tectonics. There are several lineaments in Kachchh that extend from one fault to another. Some of these also extend all the way to western boundary of Indian plate. Dynamics at plate boundaries and at fault planes determine the kinematics of basin that result in seismic activities (Sen et. al., 2019).

The city of Bhuj and its surroundings that were primary field sites for the study, lies on Kachchh Mainland Uplift (KMU) which is an upliftment caused due to formation of Kachchh Mainland Fault (KMF). This upliftment lies as a horizontal band extending from central part of Kachchh basin to nearly western coast. Katrol Hill Fault (KHF) lies to the south of Bhuj city marking the southern boundary of KMU. Both KHF and KMF are majorly E-W trending but KMF trends to NE towards the western end. The western outskirts of Bhuj mark a NW-SE trending Vigodi-Katrol Fault (VGKF) that join KHF and KMF and mark the boundary of KMU on west. While the main study area is enclosed in these regional faults, there were several local faults observed in the area, many of which were trending majorly in NE-SW direction. Banni Fault (BF) that trends in NW-SE is marked with multiple lineaments in the same direction, lies above the KMF in the north. The Banni fault is oriented in a peculiar way that bifurcates into 2 branches forming a shape of an inverted 'Y' letter extending in SE direction. The east side of Banni fault is Wagad Uplift (WU) whose north and south boundaries are marked by North Wagad Fault (NWF) and South Wagad Fault (SWF) respectively. NWF is also known as Gedi Fault (GF). Both of these (NWF and SWF) faults trend in E-W direction. SWF is the distinguishing geological feature between WU and Little rann. Further northward in the Kachchh basin is Island Belt Fault (IBF) that is trending in E-W direction. The continuity of IBF is broken multiple times by several perpendicularly trending smaller faults that shifted the fault plane of IBF north of southward making a second, strike-slip fault. These strike-slip movements have broken the continuity of upliftment caused by IBF in multiple parts thus creating smaller uplifted islands, giving the name of the fault as 'Island Belt'. There are 4 of these islands and they are named as Pachcham Uplift (PU), Khadir Uplift (KU), Bela Uplift (BU) and Chorar Uplift (CU) respectively from west to east. In the northernmost part of Kachchh an E-W trending fault is active by the name Nagar Parkar Fault (NPF). This fault is almost parallel to the political boundary between India and Pakistan. A similar strike-slip movement like IBF has moved NPF southwards and then again northwards at the western end of the fault

due to two subsequent NE-SW and NW-SE trending conjugate faults. The uplift caused by NPF is called Nagar Parker Uplift (NPU) lies north to the fault plane and hosts the Great Rann of Kachchh. The upliftment is bordered by Allah Bund Fault (ABF), another E-W trending fault that lies completely in political boundaries of Pakistan (Biswas, 2005; Sarkar et. al., 2007; Maurya et. al., 2016; Chandrasekhar et. al., 2018; Vanik et. al., 2018). All of these faults are regional that extend from 25 km to ~ 200 km and most of them trend in E-W direction. An intersection of two different faults forms a knot and triggers a fault plane to break into strike slip movement. The local faults that cause such strike-slip movement along the fault planes of the regional faults are observed to be approximately perpendicular to the regional faults and parallel to each other. All the faults and geological features observed in Kachchh basin are imaged in detail in Fig. 1.6.



# Chapter 2

## Methodology

One of the fundamental aspects in structural geology is to interpret the kinematics of faulting in rocks and their effect on tectonics of the region (Mukherjee, 2018). Faulting in rocks occur due to stresses that act on the rock body and its capacity to withstand the strain. The kinds of stresses that act on any rock body are compressional, extensional, shearing or any combination of these. Based on the acting stresses, the faults can be divided into 3 major types: normal, reverse and strike-slip faults. Although these are the major types, it is very rare to find a pure normal, reverse or strike slip fault and it usually exists as a combination of strike-slip and dip-slip (normal/reverse) faults. The slickenlines that may occur on the fault plane due to friction indicate the direction of faulting and movement of one block over another. These slickenlines are used to interpret stress axes directions that were acting on the rock body during faulting and the method is called as paleostress analysis (Delvaux et. al., 1997).

### 2.1 Data Sampling and Documentation

The study of fault planes was undertaken in the field with the agenda to perform paleostress analysis afterward. The field studies mainly focused on data sampling and documentation while analysis was performed in the later stages. The aim of the field study was to observe various types of geological structures in and around Bhuj city. The most promising and distinguishing feature observed was a fault plane on the vertical section on Kodki road towards the west of Bhuj city. The shifted sedimentary layers helped to find the direction of slip and determine that it was a normal fault. An image of this fault with different slipped sedimentary bands is shown in Fig. 1.3 (a).



Once this fault plane was located, further study included observing smaller structures surrounding this fault. A numerous small scale faults were observed in the vicinity of this major fault. The fault was exposed on a vertical section on the roadside and the plane was observed to be continued along an uplifted rock segment. The fault was also studied from the top after scaling the hillock of uplifted segment and it was observed that the top of the fault plane hosted many veins that were trending parallel to the fault plane direction. The density of number of veins increased as the distance from the fault plane was reduced, thus forming a dense interlocking network of multiple veins. The veins were also observed to be discontinuous and shifted indicating strike-slip movement almost perpendicular to the major fault plane trending direction. The strike-slip movements were also observed to be more near to the fault plane and less as the distance from the fault plane was increased. This strike-slip movement on the top of a normal fault plane indicates multiple faulting events that occurred independently at different time period. The vein network and strike slip movement visible along the veins were imaged and shown in Fig. 1.1 (b).

After identifying various features, the next step was to note characteristics of each of these features. I collected data related to the strike, dip, dip direction of each fault, and, rake of slickenlines, fractures and veins. The device used for measurements of all these properties was a Clinometer. It is a simple device used for angular measurements like slope, elevation or depression of an object with respect to the acting direction of gravity at a particular place. It has a magnetic needle and angular markings from  $0^{\circ}$  to  $360^{\circ}$  that together gives the direction of strike of any geological feature like fault or vein. Another scale on Clinometer is a similar angular scale with markings from 0 to 90 which is used to measure the slope or dip of the feature. Together these two scales can measure all necessary characteristics of a geological feature. The clinometer used in field is shown in Fig. 2.1.

The data collected from measurements for every observed structure was recorded in a notebook in the field and documented digitally afterward at the end of each day. The data was separated according to the type of structure and an image of the same was attached with it for the reference. All the data acquired from the field and used for paleostress analysis is tabulated as per the respective sites in Appendix B. The field study region was divided into multiple smaller areas and

named as area A, area B and so on, to distinguish between the observed features in each areas. Area A and B consisted the major fault observed on the Kodki road and area C, D, E was the plain land in the vicinity of the fault plane. Of these, in area E, lying to the south of area A and the fault plane, a number of smaller faults were observed with slickenlines on their exposed fault planes. This was an interesting find as the slickenlines and fault planes could be used in paleostress analysis which was done later. A similar pattern of multiple exposed fault planes with slickenlines were observed at multiple study areas, some of which were also conjugate fault systems. Area E, K, M, N and O were the sites at which such exposed fault planes with slickenlines were observed. Area O was situated along Kalo Dungar road, very far from other data acquisition sites, which were along Kodki road and the kinematics of faulting and slickenlines at area O was very different than that of other sites. A detailed map of all the sites for slickenlines data on Kodki road is shown in Fig. 2.2. Structures observed at other sites consisted of fractures caused due to weathering, multiple colour patterns formed by sedimentary rock bands, fossiliferous rock sediments and many more. These features, although very interesting, were not studied in depth as the scope of this study was limited to paleostress and inversion analysis.



Fig. 2.1: A clinometer. Source: Shutterstock.

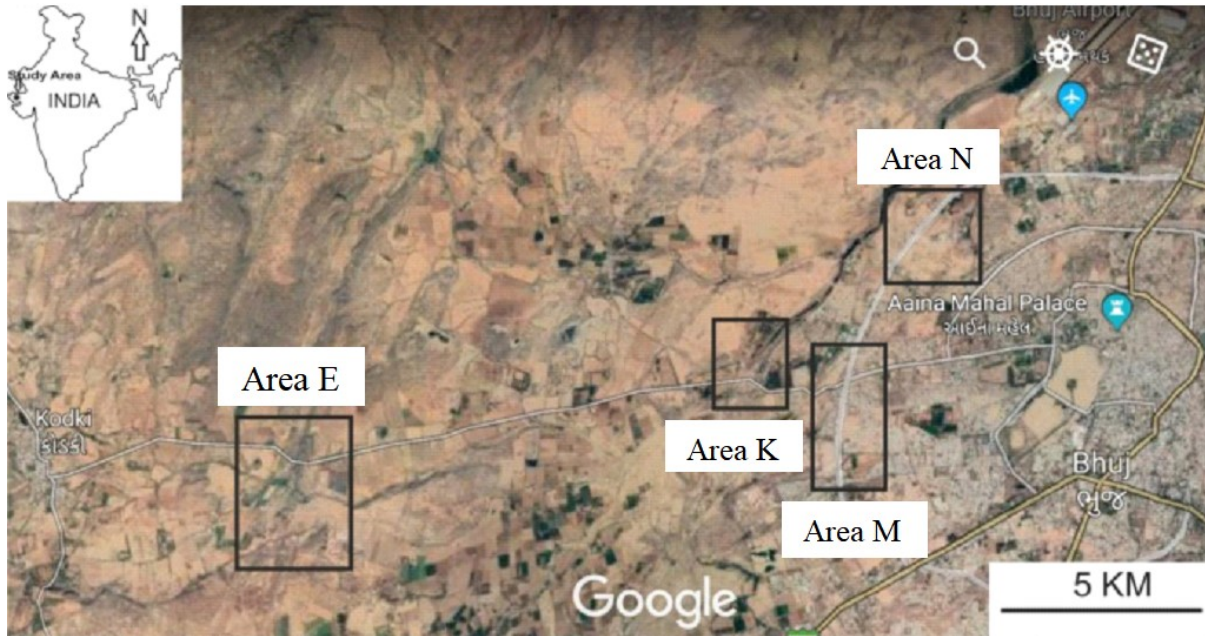


Fig. 2.2: Geological location of data acquisition sites for fault plane and slickenlines in the outskirts of Bhuj, Gujarat, India.

## 2.2 Paleostress and Inversion Analysis

To understand the deformational kinematics of Kachchh basin near Bhuj city, paleostress and inversion analysis was performed. The programs used for the same are T-TECTO (Studio X5) and Win\_Tensor (4.0). The motivation for using multiple programs instead of one was to cross verify the results from one with another, thus increasing the reliability of results from both programs. The working principle of both T-TECTO and Win\_Tensor is that it produces principle stress axes orientation directions when the input of strike, dip and rake of lineation lying on a fault plane is given. The working principles for each program are detailed in the following sections briefly and detailed in Appendix A along with their assumptions to perform the analysis.

### 2.2.1 Working principles of T-TECTO

The version used for performing analysis of the acquired fault slip data was T-TECTO Studio X5 developed in 2014. The program is developed by Dr. Jure Žalohar who also claims the copyrights of the program and a licensed copy of the same was requested from him before performing the analysis. This program is based on several innovative mathematical algorithms as mentioned below along with their developers:

1. Gauss Stress Inversion (Žalohar and Vrabec, 2007)
2. Multiple Slip Method (MSM) (Žalohar and Vrabec, 2008)
3. Cosserat Stress Strain Inversion (Žalohar and Vrabec, 2010)
4. Tectonic Wedge Faulting and Fault Interaction Theory (Žalohar 2012)

The T-TECTO Studio X5 program uses several different numerical methods as mentioned above to perform classical and micropolar analysis of heterogeneous and homogeneous fault-slip data. The basis of this analysis is the concept of best fitting stress and strain tensors (Žalohar and Vrabec, 2007). Gauss method was used to sort out heterogeneous fault-slip data into homogeneous fault subsystems and Gauss weighted RDM method was used to calculate the stress tensor. RDM is based on Anderson's theory of faulting which assumes that the orientation of maximum principle stress axis ( $\sigma_1$ ) is constrained to the (pressure) P-quadrant, and the orientation of minimum principle stress axis ( $\sigma_2$ ) is constrained to the (tension) T-quadrant associated with a chosen fault. These quadrants are defined by orientation and slip sense of fault planes. Another assumption is that faults active in the same stress field will have common intersection of P and T quadrants thus enabling the constraining and best fitting of stress tensor. T-TECTO identifies faults compatible with the calculated stress tensor with a threshold angular misfit. Appendix A summarizes step wise functioning of T-TECTO for inversion and paleostress analysis.

The compatibility function defined while performing analysis is used to verify the compatibility a given stress or strain tensor with observed fault slip data. To constrain the inversion results to mechanically acceptable solutions, T-TECTO considers the ratio of normal and shear stress on fault plane thus keeping the assumption that stress and strain inversion results are in agreement with Amonton's law. The optimal solution for stress and strain tensors are found by searching for global and highest local maxima of the object function that is defined as sum of compatibility functions for all fault slip data.

### **2.2.2 Working principles of Win\_Tensor**

Win\_Tensor is a paleostress reconstruction program developed by Dr. Damien Delvaux initially for DOS and later converted to Windows. The version of the program used was Win\_Tensor 4.0 developed in 2014. Similar to T-TECTO, a licensed copy of Win\_Tensor was also requested and used for the analysis. The methods available for constructing stress tensors are PBT axis methods and Right Dihedra Method (RDM). This study used PBT axis method in Win\_Tensor as RDM was used in T-TECTO thus giving a chance to cross verify results from both programs and using both methods.

The acquired fault data are plotted in Schmidt equal area projections and PBT axis method is used to compute stress tensor. Fault data that best fits with the results is then sorted out. This is similar to sorting of homogeneous subsystems from heterogeneous data set in T-TECTO. The fault slip data that do not fit in the angular misfit range are left out of the analysis. Win\_Tensor also obeys Anderson's theory of faulting and its assumptions, however it also obeys Bott's assumption that the slipping direction of a fault plane is towards maximum resolved shear stress (Delvaux and Sperner, 2003). The P and T quadrants are deduced from the orientation of fault plane, the slip line and the slipping sense. Appendix A shows step wise functionality of the program to perform paleostress analysis.

# Chapter 3

## Results

### 3.1 Results from T-TECTO

After performing paleostress analysis using T-TECTO, the parameters in the obtained results consisted of principle stress axes directions and their relative magnitude. The relative magnitude obtained was in percentage and was a quantitative measure of reliability, i.e. percentage of data entries that can be represented by the obtained stress axes orientations. Although it was not possible to obtain absolute values of stress magnitudes using paleostress analysis, T-TECTO provided a ratio of values of relative magnitudes of stresses, which could be used to compute the stress ratio (R), that essentially provides the shape of the stress ellipsoid (Žalohar and Vrabec, 2007). This ratio of magnitudes was in order of maximum principle stress ( $\sigma_1$ ) to intermediate principle stress ( $\sigma_2$ ) to minimum principle stress ( $\sigma_3$ ). Inversion analysis in T-TECTO also provided directions of principle strain axes that resulted from acting stresses on the rock body and the ratios of relative magnitudes of strain similar to that of principle stresses i.e. maximum ( $\varepsilon_1$ ) to intermediate ( $\varepsilon_2$ ) to minimum ( $\varepsilon_3$ ).

Along with the quantitative parameters that were obtained from T-TECTO, inversion analysis also computed a stereonet diagram with all input fault system data entries together with computed stress axes directions. The principle stress axes were marked with yellow circles, biggest for  $\sigma_1$ , intermediate for  $\sigma_2$  and smallest for  $\sigma_3$ . The diagram also consisted of hollow squares indicating principle strain directions in a similar manner, marking biggest for  $\varepsilon_1$ , intermediate for  $\varepsilon_2$  and smallest for  $\varepsilon_3$ . The stereonet was tainted in red and blue coloured circular patches dividing the net into quadrants, of which blue ones represented extensive and red ones represented compressive strain fields. This diagram also has a component that are red inward and blue outward arrows that represent direction of compressive and tensile stress

respectively. Along with these, there are black inward or outward arrows that represent direction of strain tensor. Sometimes these strain tensors can be in multiple dimensions representing multi-phase faulting in the rock body. The combined image with all these parameters make the stereonet appear as a red and blue ball with arrows on the outside and thus this diagram is called as beach ball diagram. The beach ball diagrams for each data acquisition site are shown below from Fig. 3.1 to Fig. 3.5.

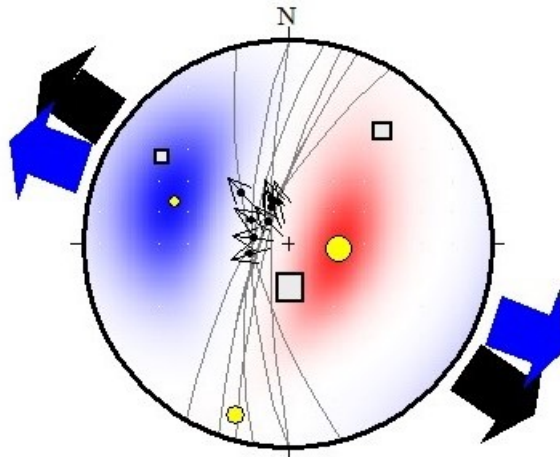


Fig. 3.1: Beach ball diagram for inversion analysis of faults observed behind hill on Kodki road, Bhuj, Gujarat (Area E). Yellow circles in the decreasing order of size represent directions of maximum, intermediate and minimum principle stress axis respectively. Similarly Square boxes represent directions of principle strain axis. The analysis is performed using T-TECTO program.

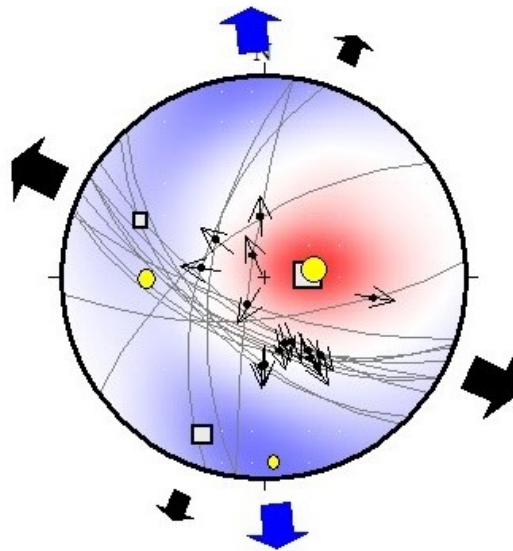


Fig. 3.2: Beach ball diagram for inversion analysis of faults observed near Khari nadi bridge, Bhuj, Gujarat (Area K). Yellow circles in the decreasing order of size represent directions of maximum, intermediate and minimum principle stress axis respectively. Similarly Square boxes represent directions of principle strain axis. The analysis is performed using T-TECTO program.

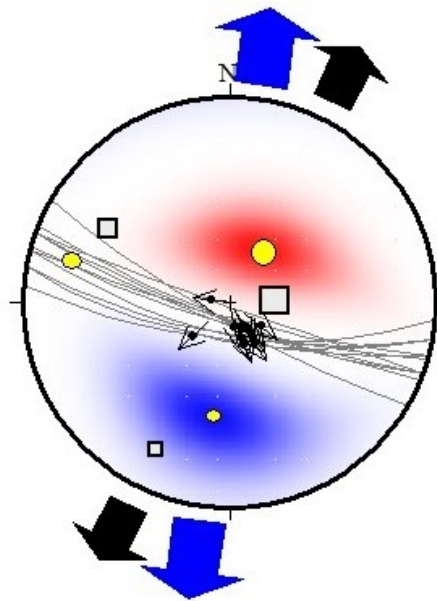


Fig. 3.3: Beach ball diagram for inversion analysis of faults observed near Trimandir area, Bhuj, Gujarat (Area M). Yellow circles in the decreasing order of size represent directions of maximum, intermediate and minimum principle stress axis respectively. Similarly Square boxes represent directions of principle strain axis. The analysis is performed using T-TECTO program.



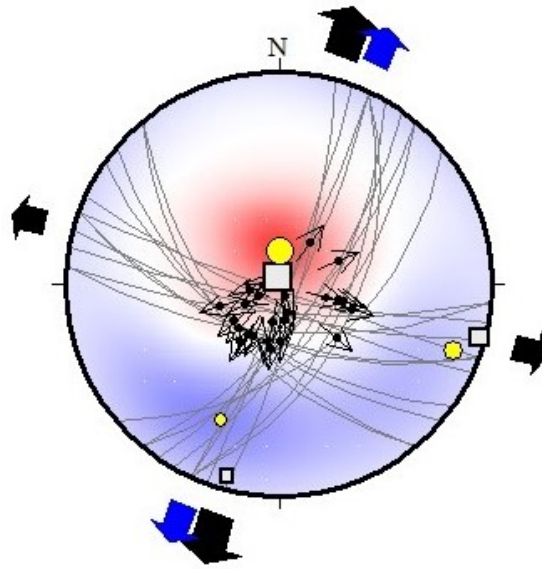


Fig. 3.4: Beach ball diagram for inversion analysis of faults observed near Motapir dargah, Bhuj, Gujarat (Area N). Yellow circles in the decreasing order of size represent directions of maximum, intermediate and minimum principle stress axis respectively. Similarly Square boxes represent directions of principle strain axis. The analysis is performed using T-TECTO program.

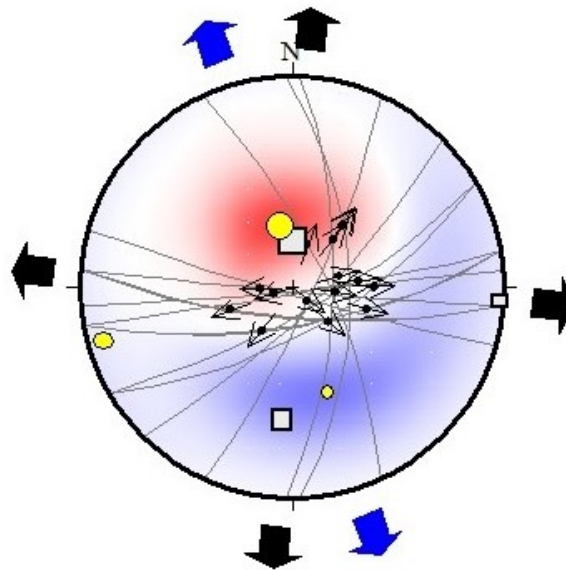


Fig. 3.5: Beach ball diagram for inversion analysis of faults observed along Kalo Dungar road, Bhuj, Gujarat (Area O). Yellow circles in the decreasing order of size represent directions of maximum, intermediate and minimum principle stress axis respectively. Similarly Square boxes represent directions of principle strain axis. The analysis is performed using T-TECTO program.

Area	Stress analysis			Strain Analysis		
	Dip Direction/Dip (Magnitude)			Dip Direction/Dip		
	$\sigma_1$ (%)	$\sigma_2$	$\sigma_3$ (%)	$\epsilon_1$	$\epsilon_2$	$\epsilon_3$
	$\sigma_1 : \sigma_2 : \sigma_3$			$\epsilon_1 : \epsilon_2 : \epsilon_3$		
Area E	96/61 (85)	197/6	290/27 (94)	176/65	40/18	305/16
	0.92 : 0.49 : 0.07			0.43 : 0 : -0.42		
Area K	81/61 (80)	269/29	177/3 (53)	89/65	201/10	295/23
	1.03 : 0.26 : 0.07			0.58 : -0.19 : -0.38		
Area M	34/57 (92)	285/12	188/30 (94)	88/65	302/21	207/12
	0.98 : 0.34 : 0.07			0.52 : -0.12 : -0.39		
Area N	2/71 (74)	111/6	203/19 (46)	0/86	105/1	195/4
	0.99 : 0.16 : 0.07			0.58 : -0.25 : -0.34		
Area O	349/56 (74)	254/3	162/33 (51)	2/65	184/25	94/1
	1.06 : 0.08 : 0.08			0.65 : -0.33 : -0.33		

Table 3.1: Results of inversion analysis performed in T-TECTO using Gauss weighted RDM.

## 3.2 Results from Win\_Tensor

Another program that was used for paleostress and inversion analysis was Win\_Tensor, the results of which consisted of quantitative parameters of principle stress axes orientations but did not reveal the same for principle strain axes. The difference between result parameters from T-TECTO and Win\_Tensor was that T-TECTO did not give stress ratio (R) values as opposite to Win\_Tensor. Win\_Tensor also provided computed values of stress regime index (R') which along with stress ratio was used to understand the type of stress acting on the rock body. Along with these parameters, Win\_Tensor also computed principle stress axes orientations similar to T-TECTO. The rose diagrams of strike, dip, plunge and plane of faulting were also constructed in Win\_Tensor.

The stereonet consisting of fault planes and slickenlines data also incorporated girdles of most probable orientation of all three principle stress axes. The stress axes were marked by small yellow circles and the distinction between maximum ( $\sigma_1$ ), intermediate ( $\sigma_2$ ), and minimum ( $\sigma_3$ ) principle stress axes was denoted by circle, triangle and square respectively encircling the small yellow circle. The planes of probable P, B and T axes deduced from the computed inversion analysis were also plotted along with the stereonet (Delvaux and Sperner, 2003). As similar to T-TECTO, the stereonet from Win\_Tensor also had red arrows pointing outwards indicating the direction of applied extension. The stereonet however was

not divided into compressional and extensional strain fields similar to that in T-TECTO.

The results of inversion and paleostress analysis for the same data set as computed from two different programs was then compared and the results were found out to be very similar. The variability of results can be accounted by the different algorithms used in the two programs. The results for stress axes orientations obtained from T-TECTO and Win\_Tensor are tabulated in Table 3.1 and Table 3.2 respectively. Stereonet diagrams for inversion analysis of faults in Win\_Tensor from various data acquisition sites are shown below from Fig. 3.6 to Fig. 3.10.

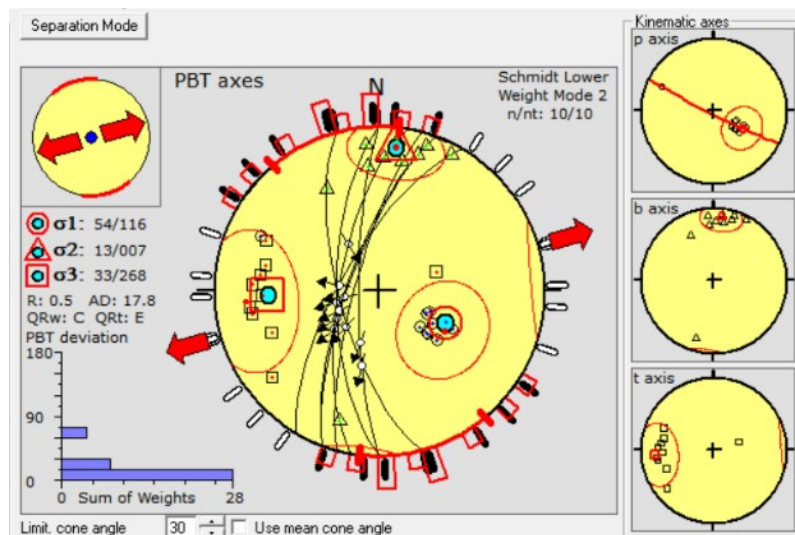


Fig. 3.6: Stereonet with great circles for fault planes and directions of principle stress axes. Great circles for P, B and T axes in right panel. Stress regime in inset on top left. Numerical values of directions of stress axes are given on left side. Data collected from hill on Kodki road, Bhuj, Gujarat (Area E). The analysis is performed using Win\_Tensor program.

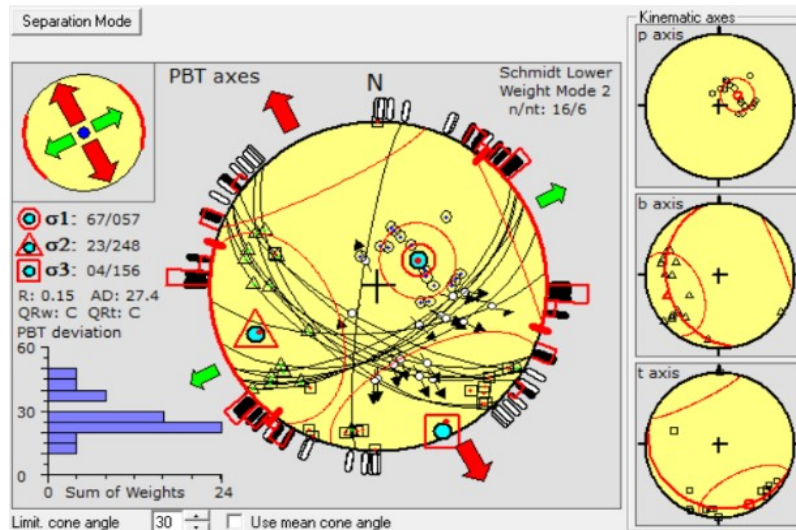


Fig. 3.7: Stereonet with great circles for fault planes and directions of principle stress axes. Great circles for P, B and T axes in right panel. Stress regime in inset on top left. Numerical values of directions of stress axes are given on left side. Data collected from Khari nadi bridge, Bhuj, Gujarat (Area K). The analysis is performed using Win\_Tensor program.

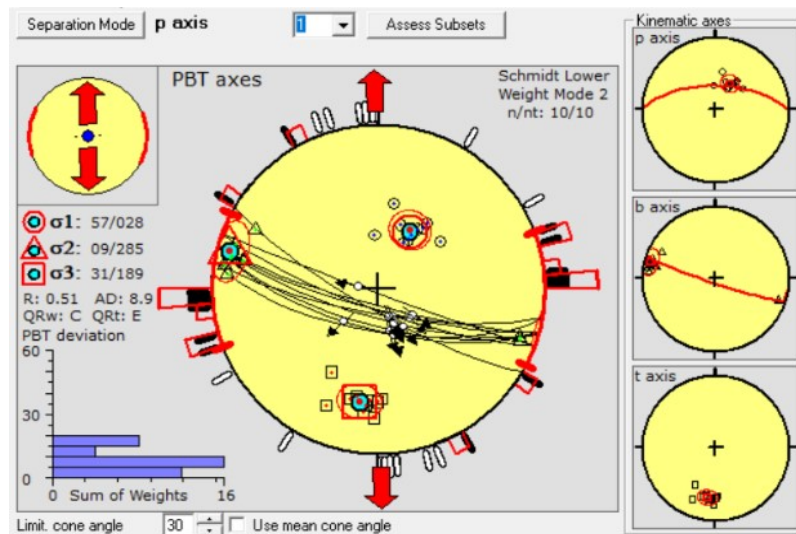


Fig. 3.8: Stereonet with great circles for fault planes and directions of principle stress axes. Great circles for P, B and T axes in right panel. Stress regime in inset on top left. Numerical values of directions of stress axes are given on left side. Data collected near Trimandir, Airport road, Bhuj, Gujarat (Area M). The analysis is performed using Win\_Tensor program.

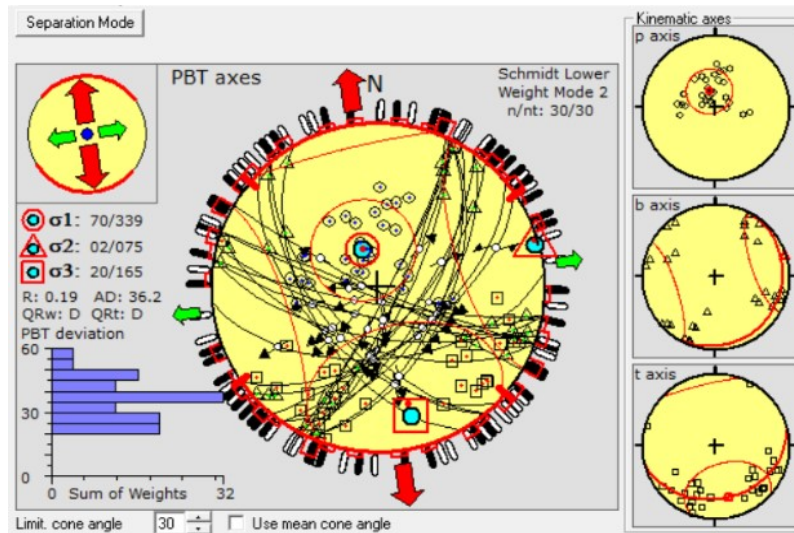


Fig. 3.9: Stereonet with great circles for fault planes and directions of principle stress axes. Great circles for P, B and T axes in right panel. Stress regime in inset on top left. Numerical values of directions of stress axes are given on left side. Data collected from Motapir dargah hill, Airport road, Bhuj, Gujarat (Area N). The analysis is performed using Win\_Tensor program.

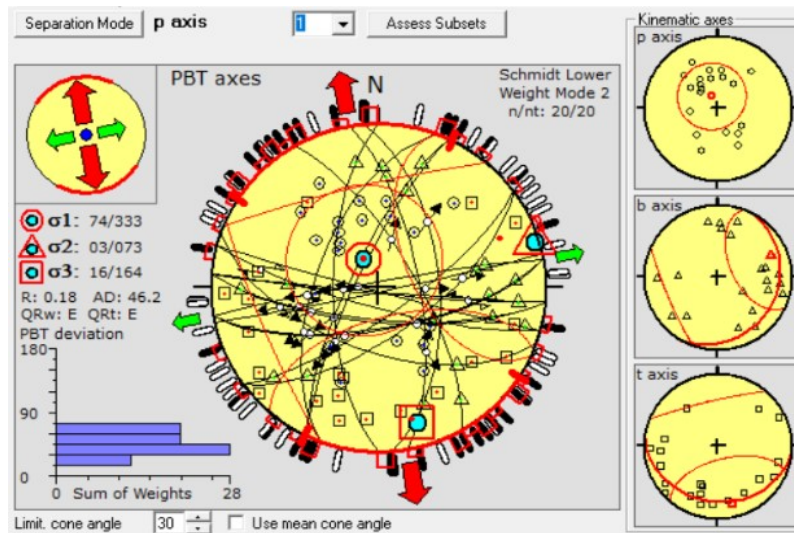


Fig. 3.10: Stereonet with great circles for fault planes and directions of principle stress axes. Great circles for P, B and T axes in right panel. Stress regime in inset on top left. Numerical values of directions of stress axes are given on left side. Data collected from various sites on Kalo Dungar road, Bhuj, Gujarat (Area O). The analysis is performed using Win\_Tensor program.

Area	Stress Analysis			Stress Ratio	Stress Regime Index
	Dip/Dip Direction				
	$\sigma_1$	$\sigma_2$	$\sigma_3$	R	R'
Area E	54/114	13/007	33/268	0.5	0
Area K	67/057	23/248	4/156	0.15	0.5
Area M	57/028	09/285	31/189	0.51	0.5
Area N	70/339	02/075	20/165	0.19	0.5
Area O	74/333	03/073	16/164	0.18	0.5

Table 3.2: Results of inversion analysis performed in Win\_Tensor using PBT axes method.

# Chapter 4

## Discussions

### 4.1 Comparative analysis of results from T-TECTO and Win\_Tensor

When the paleostress analysis was performed using Gauss weighted RDM method in T-TECTO and using PBT axes method in Win\_Tensor, the results obtained were compared and were found to be very similar. The principle stress axes orientations calculated for each data sets from both softwares were found to be approximately similar. Table 4.1 shows comparison between results of  $\sigma_1$ ,  $\sigma_2$  and  $\sigma_3$  obtained from both programs. From the table it can be observed that in most of the results the variation in dip is around 10 and that in dipping direction is around 20-25 degrees. The variability in results can be accounted by difference in the methods used and its assumptions while performing the analysis using the algorithm.

Area	$\sigma_1$ results (Dip/DD)		$\sigma_2$ results (Dip/DD)		$\sigma_3$ results (Dip/DD)	
	T-TECTO	Win_Tensor	T-TECTO	Win_Tensor	T-TECTO	Win_Tensor
E	61/96	54/114	6/197	13/007	27/290	33/268
K	61/81	67/057	29/269	23/248	3/177	4/156
M	57/34	57/028	12/285	09/285	30/188	31/189
N	71/002	70/339	6/111	02/075	19/203	20/165
O	56/349	74/333	3/254	03/073	33/162	16/164

Table 4.1: Comparative analysis of stress axes orientations from T-TECTO and Win\_Tensor.

## 4.2 Stress ratio and Stress regime

The arrows and circles from beach ball diagrams gives the orientation of principle stress axes, but, they don't provide any information regarding the stress regime that the deformation belongs to. Hence to gain an insight into the stress regime of faulting, calculation of stress ratio is required. Stress ratio is a mathematical formulation that uses relative magnitudes of principle stresses to give a number that determines the regime of stress that the deformed rock body belongs to. The mathematical formula for calculation of stress ratio is given in Eq. 1.

$$R = (\sigma_2 - \sigma_3) / (\sigma_1 - \sigma_3) \quad \text{Eq. 1}$$

The value of stress ratio defines the shape of stress ellipsoid (Delvaux et. al., 1997). The stress regime is determined by the nature of vertical stress axis ( $S_v$ ). Stress regime is extensional when  $\sigma_1$  is vertical, strike-slip when  $\sigma_2$  is vertical and compressional when  $\sigma_3$  is vertical respectively (Angelier, 1989). Among these 3 major types the stress regime is again sub divided into 7 different types and these are determined using stress ratio values. The stress act in radial extension when  $\sigma_1$  is vertical and  $0 < R < 0.25$ , in pure extension when  $\sigma_1$  is vertical and  $0.25 < R < 0.75$ , in transtension when  $\sigma_1$  is vertical and  $0.75 < R < 1$  or  $\sigma_2$  is vertical and  $1 > R > 0.75$ , in pure strike slip when  $\sigma_2$  is vertical and  $0.75 > R > 0.25$ , in transpression when  $\sigma_2$  is vertical and  $0.25 > R > 0$  or  $\sigma_3$  is vertical and  $0 < R < 0.25$ , in pure compression when  $\sigma_3$  is vertical and  $0.25 < R < 0.75$  and in radial compression when  $\sigma_3$  is vertical and  $0.75 < R < 1$  (Delvaux et. al., 1997). All these sub types are explained in Table 4.2. A descriptive explanation of all these types is illustrated in Fig. 4.1. The type of stress regime among the major 3 types can be expressed numerically using an index  $R'$  that ranges from 0 to 3.0 and is defined using following set of equations.

$$R' = R \quad \text{Extensional Stress Regime } (\sigma_1 \text{ is vertical}) \quad \text{Eq. 2}$$

$$R' = 2 - R \quad \text{Strike-slip Stress Regime } (\sigma_2 \text{ is vertical}) \quad \text{Eq. 3}$$

$$R' = 2 + R \quad \text{Compressional Stress Regime } (\sigma_3 \text{ is vertical}) \quad \text{Eq. 4}$$



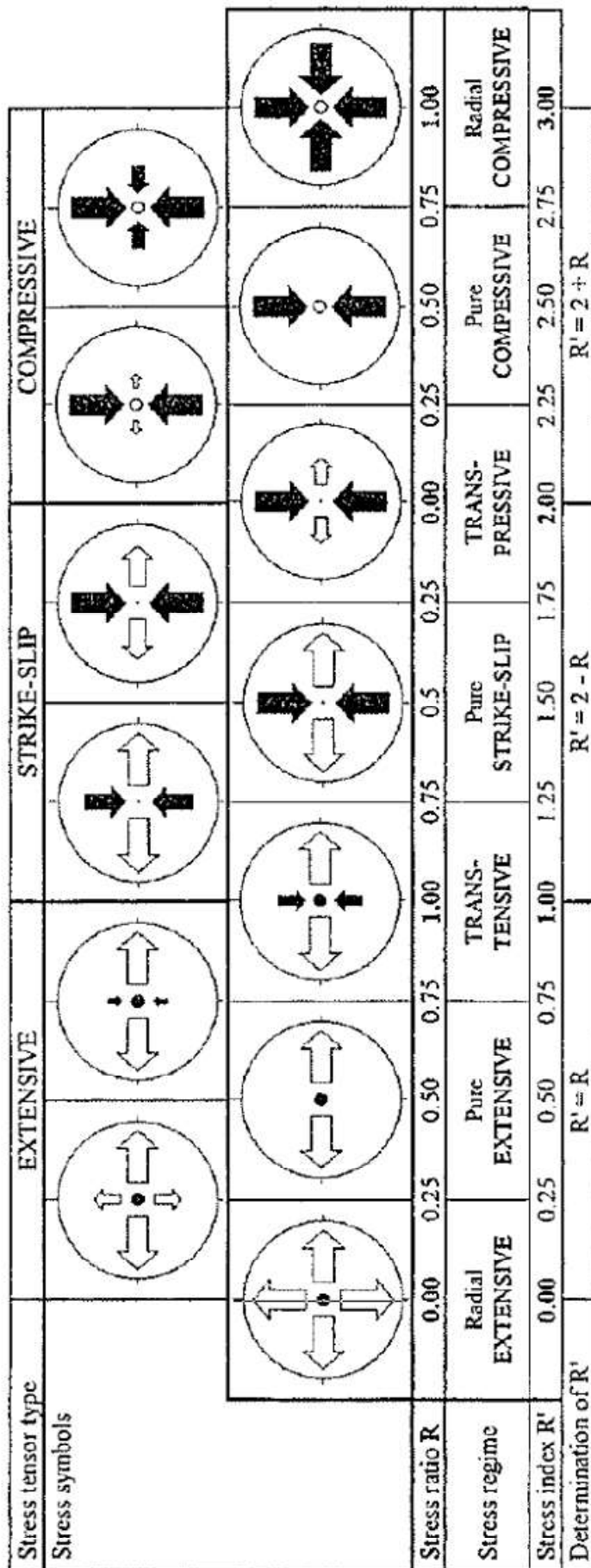


Fig. 4.1: Illustration of types of stress regimes, meaning of stress regime index  $R'$  versus  $R$  and variation of stress regimes with respect to it. Stress symbols with horizontal stress axes ( $S_{Hmax}$  and  $S_{Hmin}$ ), as a function of stress ratio. The length and colour of stress symbols indicate horizontal deviatoric stress magnitude, relative to isotopic stress ( $\sigma_i$ ). White outward arrows show extensional deviatoric stress ( $<\sigma_i$ ), black inward arrows show compressional deviatoric stress ( $>\sigma_i$ ) and vertical stress ( $\sigma_v$ ) is symbolized for extensional regimes by solid circle ( $\sigma_1 = \sigma_v$ ), for strike slip regimes by a dot ( $\sigma_2 = \sigma_v$ ) and for compressional regimes by an open circle ( $\sigma_3 = \sigma_v$ ). Reproduced from Delvaux et. al. (1997).

<b>Stress regime</b>	<b>Vertical stress axis</b>	<b>R value range</b>
Radial Extension	$\sigma_1$	0 - 0.25
Pure Extension	$\sigma_1$	0.25 - 0.75
Transtension	$\sigma_1$ Or $\sigma_2$	0.75 - 1 Or 1 - 0.75
Pure Strike Slip	$\sigma_2$	0.75 - 0.25
Transpression	$\sigma_2$ Or $\sigma_3$	0.25 - 0 Or 0 - 0.25
Pure compression	$\sigma_3$	0.25 - 0.75
Radial Compression	$\sigma_3$	0.75 - 1

Table 4.2: Stress regime type variation according to Vertical stress axis and R value.

### 4.3 Stress regime and Fault formation timeline

The Kachchh rift basin was formed after the Indian plate broke off from Gondwanaland in the Mesozoic period (Maurya, 2000). Before the Indian plate collided with Eurasian and Arabian plate on the west, the basin was under extensional stress. After collision of the Indian plate on Eurasian plate, the extensional regime of KRB was overturned to be compressional (Biswas, 1987). This collision that caused the stress orientation change took place approximately around  $55 \pm 1$  Million years ago. The orientation of the compressional stress regime was N-S trending. Many of the normal faults observed on KRB are supposed to be formed under extensional regime, i.e. before  $55 \pm 1$  Ma and the reverse faults under compressional regime after  $55 \pm 1$  Ma (Vanik et. al., 2018). As the compressional stress fields were oriented in N-S direction, most of the reverse faults observed on KRB are E-W trending and normal faults approximately NW-SE or N-S trending.

The fault planes and slickenlines data acquired from field study indicated that most of the faults observed were N-S trending although all of them were normally faulted. This observation, along with consideration of other major normal fault orientations can reason out that the stress regime before the collision could possibly be radial instead of pure extensive. This speculation, however, cannot be concluded only from the data acquired for this study. However, the results from Win\_Tensor

suggests that for area E and area M, the stress regime is pure extensive and that for area K, area M and area N, is radially extensive.

The fault slip data from various locations, after paleostress analysis concluded that the extensive stress tensor direction is predominantly in N-S direction, and most of the faults are oriented in NNW-SSE direction. For extensive regime, the vertical stress axis ( $\sigma_v$ ), is determined by  $\sigma_1$ , as understood from Fig. 4.1 (Delvaux et. al., 1997). The results of paleostress analysis from Win\_Tensor and T-TECTO reveal that  $\sigma_1$  is the axis of maximum stress. Thus it can be noticed that the maximum stress acting on the deformation is acting in the vertical direction. This reasons the formation of uplifts in normally faulted rocks acting under extensional stress.

The tectonic evolution and the shape of the Kachchh peninsula and KRB is a result of regional events of breakup of Indian plate on the western margin during the separation from Gondwanaland and rapid northward drift resulting in collision with Eurasian plate (Yoshida and Hamano, 2015). This process spanned a total time period of approximately 160 My. The most rapid movement of Indian plate ( $\sim 20$  cm/yr) was during 67-52 Ma time period (Chatterjee and Bajpai, 2016). This time frame consisted of events like Deccan volcanism and post trappean intrusions. The rise of reunion plume could be reasoned for the acceleration provided for the rapid movement of the Indian plate (Yoshida and Hamano, 2015). The rise of reunion plume is also responsible for Deccan volcanism and thinning of crustal thickness. From  $\sim 55$  to 52 Ma, the motion of the plate was gradually slowed down ( $\sim 5$  cm/yr) due to onset of India-Asia collision (Gowd, 1992).

As mentioned above, most of the faults observed are normal, and paleostress analysis concludes that they are formed under extensional regime. The stress orientation history of KRB reveals that extensional regime was overturned to compressional around  $55 \pm 1$  Ma. Thus it can be hypothesized that the observed faults are possibly formed before the Indian plate collided with Eurasian plate (before  $55 \pm 1$  Ma). The KRB suffered significant tectonic activity during the northward movement after breakup from Gondwanaland and also during collision with Eurasian plate (Maurya, 2000). The transition of stress regime from extensional to transpressional to compressional occurred only after the collision and enduring till date in northern Kachchh.

Many of the faults generated by extensional stress were reactivated during the transition of stress regime and continued to do so even later as the same stress

scenario continued to exist through most of the Cenozoic period (Biswas, 1987). This reactivation is observed in most of the regional faults (like KHF, KMF, Katar Fault in Saurashtra) in highly fragmented western continental margin of India including KRB and Saurashtra region (Mukherjee, 2018). The recent earthquake history in Kachchh (near Bhuj) and Saurashtra (near Rajula) also suggests the neotectonically active environment in and around the faults in KRB (De et. al., 2003; Mandal et. al. 2007; Mandal, 2009). A further detailed study in the vicinity of these faults can fully comprehend the deformation history and fault reactivation kinematics during and after compressional stress regime in KRB. This will link the studied faults along with other observed faults in KRB to neotectonic evolution of the basin.

# Chapter 5

## Conclusions

The present study has led to following conclusions:

1. A previously unmapped fault, trending in ~ N-S direction is investigated in western outskirts of Bhuj, Gujarat which revealed the fault to be faulted normally with some strike slip movement as well. The site of observation was the hill on Kodki road (Area E). Numerous other faults were also observed in other sites (Area K, M and N) that were trending in majorly E-W direction with normal faulting.
2. Many veins and vein networks were observed to be trending parallel to the strike of the fault and the density was high in the close vicinity of fault and low as the distance increased. On close observation of each vein, it came to the light that continuity of many of these veins was broken and they appeared to have shifted slightly, thus proving the strike slip movement. Most of the veins were observed to have slipped in Dextral sense.
3. On performing the paleostress analysis It was found that  $\sigma_1$  direction for Area E and Area K was towards ~ E and that for Area M and Area N was towards ~NNE.  $\sigma_3$  direction for Area E was ~W and that for Area K, M and N was ~ S.
4. All of the faults were formed under extensional stress regime as inferred from paleostress analysis. The extensional regime was induced by breakup of Indian plate from Gondwanaland until collision with Eurasian plate. Thus the faults can be assumed to have formed before the collision, although tectonic activity due to collision and recurring earthquakes have made the faults reactivate several times in past.
5. The reactivation of these faults due to collision of the plates was not included in the scope of this study and thus, further study is required to understand the neotectonic evolution and effect of recent and recurring earthquakes on these faults.

# Appendix A

## T-TECTO

Analysis in T-TECTO is performed in two steps, first is inverse analysis of faults and second is RDM analysis. RDM analysis is performed only after performing inverse analysis of faults. After entering the fault slip data and checking for errors, the data is saved and Gauss method is selected in 'Method' drop down box. The saved data set is then selected for inverse analysis of faults from 'Tools' box.

In inverse analysis of faults, analysis of phase 1 is selected to check the compatibility of the data and maximum angle is set to exclude misfit data from the homogeneous subset. After this, analysis of phase 2 is performed to get results of associated faults to the homogeneous subsystem and problematic faults to the same. The inverse analysis box is then closed and RDM is set checked from 'Tools' box after strain page is selected. The visualization preferences are set in the opened dialogue box and the box is closed. The results are calculated after setting inversion (stress) box checked in the right corner of the program. The computation takes a few minutes to perform the analysis after which results are displayed in bottom right corner and beach ball diagram in top left corner. This image of beach ball diagram can be copied directly and used for publishing results, however the numerical results of orientation of principle stress axes need to be noted down manually. The additional information regarding the set parameters can be found in statistics page. The Mohr diagram, problematic faults and histograms associated with the result can be found and copied from the respective pages.

## Win\_Tensor

Analysis in Win\_Tensor is performed in only one step, but the program is organized in two linked windows: a data worksheet and a processing worksheet. The data worksheet is the one in which all the input data is fed to the program and is saved in the same. The processing worksheet performs the sorting of heterogeneous data entries from the homogeneous subsystems and further analysis.

The entry of all the data points is done manually or can be copied from a different source in a specific format. Win\_Tensor assigns unique format code for entering the data of planes and lines. This is explained in Table A1. After entering all data in the worksheet, the file is saved and the processing worksheet is opened.

Format Index	First Digit: Format for planes	Second digit: Format for lines
11	1: Dip / Dip Direction	1: Plunge / Azimuth
22	2: Dip Direction / Dip	2: Azimuth / Plunge
33	3: Strike (0°-180°) / Dip (N,E,S,W)	3: Pitch or Trend (with N,E,S,W)
44	4: Strike (0°-360°) / Dip (0°-90°)	4: Rake or Slip (0°-360°)

Table A1: Format code for entering data in Win\_Tensor data worksheet.

The processing worksheet gives results of the heterogeneous set of all entered data points combined at first. Due to this data separation is mandatory. To sort out homogeneous set of faults, in the data icon, 'set minor index for rejected data' is selected. This opens a dialogue box, assigning a minor index for misfitting data entries. The PBT axes page is selected, which shows a box for data separation. In this box, the threshold for rejecting data is selected and on clicking next, the misfit entries are transferred to assigned index. A PBT deviation graph is shown along with the data separation box. The separation of data is considered adequate if the PBT deviation is below 30. The indices of separated data sets are given in left panel in the processing worksheet.

As the data is being separated, the paleostress analysis is performed simultaneously in the right panel. The results are changed as the data is separated into homogeneous subsets. Once the data separation is done, the final results of orientation of principle stress axes are noted and the stereonet diagram is copied to be documented. The stereonet also includes the stress regime of deformation and individual P, B and T kinematic axes in individual stereonets. The parameters like stress ratio (R) and stress regime index (R') can be found along with principle stress axes orientations in results panel. The rose diagrams for strike, dip and plunge of all fault entries can be copied from rose diagram page and Mohr circle is also found in the respective page.

# Appendix B

## Fault Slip data used for the study

The data sampled from the field and used for paleostress analysis is tabulated below according to the sites of sampling.

Fault plane attitude				Lineation attitude		Rake (w.r.t. RHS of Strike)
Strike (LHS) (in degrees)	Strike (RHS) (in degrees)	Dip (in degrees)	Dip Direction (in degrees)	Trend (in degrees)	Plunge (in degrees)	(in degrees)
10	<b>190</b>	70	315	234	63	70
10	<b>190</b>	69	310	232	60	68
11	<b>191</b>	68	313	256	66	80
30	<b>210</b>	71	340	280	70	83
0	<b>180</b>	69	280	303	65	103
20	<b>200</b>	75	300	263	73	82
20	<b>200</b>	74	285	245	68	74
15	<b>195</b>	78	288	346	66	111
0	<b>180</b>	80	240	339	64	115
345	<b>165</b>	70	260	317	52	123
15	<b>195</b>	80	285	349	68	110
15	<b>195</b>	78	290	318	76	98
25	<b>205</b>	80	300	319	79	95
15	<b>195</b>	70	280	319	66	103

Table B1: Data from hill on Kodki road, Bhuj (Area E)



Fault plane attitude				Lineation attitude		Rake (w.r.t. RHS of strike)
Strike (LHS) (in degrees)	Strike (RHS) (in degrees)	Dip (in degrees)	Dip Direction (in degrees)	Trend (in degrees)	Plunge (in degrees)	(in degrees)
8	<b>188</b>	82	300	342	72	106
317	<b>137</b>	54	225	180	44	58
289	<b>109</b>	70	200	157	65	73
289	<b>109</b>	74	204	147	65	70
289	<b>109</b>	60	210	192	60	86
314	<b>134</b>	50	220	183	42	60
295	<b>115</b>	60	200	163	53	66
265	<b>85</b>	67	165	100	32	35
305	<b>125</b>	68	210	149	45	49
288	<b>108</b>	72	205	212	71	94
300	<b>120</b>	55	210	150	36	45
287	<b>107</b>	52	203	148	41	55
300	<b>120</b>	58	207	168	50	64
301	<b>121</b>	65	195	268	50	122
290	<b>110</b>	55	195	245	45	120
303	<b>123</b>	68	200	280	45	130

Table B2: Data from Khari nadi bridge, Kodki road, Bhuj (Area K)

Fault plane attitude				Lineation attitude		Rake (w.r.t. RHS of strike)
Strike (LHS) (in degrees)	Strike (RHS) (in degrees)	Dip (in degrees)	Dip Direction (in degrees)	Trend (in degrees)	Plunge (in degrees)	(in degrees)
285	<b>105</b>	82	190	126	68	70
285	<b>105</b>	72	193	148	65	72
286	<b>106</b>	74	193	164	72	80
285	<b>105</b>	70	200	240	63	108
290	<b>110</b>	68	204	226	66	100
290	<b>110</b>	72	197	167	69	79
287	<b>107</b>	76	205	219	75	95
280	<b>100</b>	69	190	172	68	83
290	<b>110</b>	78	196	153	73	78
292	<b>112</b>	80	205	138	67	70
293	<b>113</b>	83	205	139	75	76

Table B3: Data from exposure near Trimandir, Airport road, Bhuj (Area M)

Fault plane attitude				Lineation attitude		Rake (w.r.t. RHS of strike)
Strike (LHS) (in degrees)	Strike (RHS) (in degrees)	Dip (in degrees)	Dip Direction (in degrees)	Trend (in degrees)	Plunge (in degrees)	(in degrees)
280	<b>100</b>	82	189	244	78	100
285	<b>105</b>	75	190	220	74	97
290	<b>110</b>	60	207	181	59	80
290	<b>110</b>	58	208	194	58	86
280	<b>100</b>	75	185	256	57	120
205	<b>25</b>	55	110	104	55	84
290	<b>110</b>	85	200	260	81	98

230	<b>50</b>	60	140	115	58	77
300	<b>120</b>	88	203	297	60	120
205	<b>25</b>	55	115	108	55	86
195	<b>15</b>	79	105	37	61	64
200	<b>20</b>	85	110	155	83	95
205	<b>25</b>	85	115	192	70	110
220	<b>40</b>	70	130	188	56	118
205	<b>25</b>	80	115	173	72	106
210	<b>30</b>	65	120	106	65	84
315	<b>135</b>	55	215	170	40	51
240	<b>60</b>	50	155	145	50	86
290	<b>110</b>	85	195	271	76	103
280	<b>100</b>	65	185	228	59	108
280	<b>100</b>	75	185	172	75	85
265	<b>85</b>	54	180	239	31	140
320	<b>140</b>	60	230	217	59	83
160	<b>340</b>	55	70	52	54	80
215	<b>35</b>	60	125	140	59	98
200	<b>20</b>	75	110	178	55	123
325	<b>145</b>	65	225	172	45	50
215	<b>35</b>	70	130	67	56	62
230	<b>50</b>	75	130	105	72	80
245	<b>65</b>	60	140	81	26	30

Table B4: Data from Motapir Dargah hill, Airport road, Bhuj (Area N)

Fault plane attitude				Lineation attitude		Rake (w.r.t. RHS of strike)
Strike (LHS) (in degrees)	Strike (RHS) (in degrees)	Dip (in degrees)	Dip Direction (in degrees)	Trend (in degrees)	Plunge (in degrees)	(in degrees)
234	<b>54</b>	76	136	89	67	72
235	<b>55</b>	66	145	85	48	54
275	<b>95</b>	87	180	99	45	45
175	<b>355</b>	60	83	36	49	60
258	<b>78</b>	85	169	253	49	130
205	<b>25</b>	76	135	55	64	68
285	<b>105</b>	85	200	261	79	100
275	<b>95</b>	74	185	250	55	121
275	<b>95</b>	87	180	267	72	107
260	<b>80</b>	70	170	235	49	126
290	<b>110</b>	58	195	260	39	131
200	<b>20</b>	59	100	125	59	98
286	<b>106</b>	80	190	279	34	145
275	<b>95</b>	73	180	134	64	70
260	<b>80</b>	88	170	82	56	55
170	<b>350</b>	70	260	144	50	125
150	<b>330</b>	72	65	14	65	73
260	<b>80</b>	69	155	217	61	110
205	<b>25</b>	79	115	39	49	50
180	<b>360</b>	68	88	37	56	64
284	<b>104</b>	85	190	130	80	80

Table B5: Data from various locations along Kalo Dungar road, Bhuj (Area O)

# References

Angelier, J. (1989). From orientation to magnitudes in paleostress deformations using fault slip data. *Journal of Structural Geology* 11, 37-50.

Biswas, S.K. (1987). Regional tectonic framework, structure and evolution of the western margin basins of India. *Tectonophysics* 135, 307-327.

Biswas, S.K. (2005). Structure and tectonics of Kutch Basin, Western India, with special reference to earthquakes. *Current Science*. 88.

Bons, P. (2000). The formation of veins and their micro-structures. *Journal of The Virtual Explorer*, 02.

Bose, N., Mukherjee, S. (2017). Map interpretation of structural geologists.

Chandrasekhar, P., Chandra Mouli, K., Rao, D.P., Dadhwal, V.K. (2018). Subsurface geological structure and tectonics as evidenced from integrated interpretation of aeromagnetic and remote sensing data over Kutch sedimentary basin, western India. *Current Science* 114, No. 1, 174-185.

Chatterjee, S., Bajpai, S. (2016). India's northward drift from Gondwana to Asia during the late Cretaceous-Eocene. *Proceedings of the Indian National Science Academy* 82 (3), 479-487.

Chopra, S., Kumar, D., Rastogi, B.K., Choudhury, P., Yadav, R.B.S. (2013). Estimation of seismic hazard in Gujarat region, India. *Natural Hazards* 65, 1157-1178.

De, R. Gaonkar, S.G., Srirama, B.V., Ram, S., Kayal, J.R. (2003). Fault plane solutions of the January 26<sup>th</sup>, 2001 Bhuj earthquake sequence. *Journal of Earth System Science*, 112, 413-419.

Delvaux, D., Moeys, R., Stapel, G., Petit, C., Levi, K., Miroshnichenko, A., Ruzhich, V., San'kov, V. (1997). Paleostress reconstructions and geodynamics of Baikal region, central Asia, Part 2. Cenozoic rifting. *Tectonophysics* 282 (1997), 1-38.

- Delvaux, D., Sperner, B. (2003). Stress tensor inversion from fault kinematic indicators and focal mechanism data: the TENSOR program. Geological Society of London Special Publication, 212, 75-100.
- Fossen, H. (2016). Structural Geology.
- Gowd, T.N., Rao, S.V. (1992). Tectonic stress field in the Indian subcontinent. Journal of Geophysical Research 97, 11879-11888.
- Heidbach, O., Rajabi, M., Reiter, K., Ziegler, M., and Team WSM (2016). World Stress Map Database Release 2016.
- Hobbs, B. (1993). The significance of structural geology in rock mechanics. Comprehensive rock engineering. Vol. 1, 25-62.
- Mandal, P., Chada, R.K., Raju, I.P., Kumar, N., Satyamurty, C., Narsaiah, R. (2007). Are the 7 March 2006 Mw 5.6 event and the 3 February 2006 Mw 4.58 event triggered by the five years continued occurrence of aftershocks of the 2001 Mw 7.7 Bhuj event? Current Science 92, No. 8, 1114-1124.
- Mandal, P. (2009). Estimation of static stress changes after 2001 Bhuj earthquake: implications towards the northward spatial migration of the seismic activity in Kachchh Gujarat. Journal Geological Society of India, Vol. 74 (2009), 487-497.
- Maurya, D.M. (2000). History of tectonic evolution of Gujarat alluvial plains, western India during Quaternary: a review. Journal of Geological Society of India 55, 343-366.
- Maurya, D.M., Chowksey, V., Patidar, A.K., Chamyal, L.S. (2016). A review and new data on neotectonic evolution of active faults in the Kachchh basin, Western India: legacy of post Deccan Trap tectonic inversion. Geological Society, London, Special Publications 445, 237-268.
- Merh, S.S. (1995). Geology of Gujarat. Geological Society of India, 106-130.
- Mukherjee, S. (2018). Tectonics and structural geology: Indian context.
- Rey, P. (2016). Introduction to Structural Geology.
- Sarkar, D., Sain, K., Reddy, P.R., Catchings, R.D., Mooney, W.D. (2007). Seismic-reflection images of the crust beneath the 2001 M = 7.7 Kutch (Bhuj) epicentral region, western India. Geological Society of America Special Papers 2007;425; 319-327.

Sen, S., Kundan, A., Kalpande, V., Kumar, M. (2019). The present-day state of tectonic stress in the offshore Kutch-Saurashtra basin, India. *Marine and Petroleum Geology* 102 (2019), 751-758.

Shaikh, M.A., Maurya, D.M., Mukherjee S., Vanik, N.P., Padmalal, A., Chamyal, L.S. (2020). Tectonic evolution of the intra-uplift Vigodi-Gugriana-Khirastra-Netra Fault System in the seismically active Kachchh rift basin, India: Implications for the western continental margin of the Indian plate. *Journal of Structural Geology* (2020).

Singh, B., Mandal, P. (2020). Upper mantle seismic anisotropy beneath the Kachchh rift zone, Gujarat, India, from shear wave splitting analysis. *Journal of Earth System Science* (2020)129, 110.

Vanik, N., Shaikh, M.A., Mukherjee, S., Maurya, D.M. (2018). Post-Deccan trap stress reorientation under transpression: Evidence from fault slip analysis from SW Saurashtra, Western India. *Journal of Geodynamics* 121 (2018), 9-19.

Woodward, N., Boyer, S., Suppe, J. (1989). Balanced geological cross sections: An essential technique in geological research and exploration.

Yoshida, M., Hamano, Y. (2015). Pangaea breakup and northward drift of the Indian subcontinent reproduced by a numerical model of mantle convection. *Scientific Reports* 5, 8407.

Žalohar, J., Vrabec, M. (2007). Paleostress analysis of heterogeneous fault slip data: The Gauss Method. *Journal of Structural Geology* 29 (2007), 1798-1810.